J Therm Anal Calorim (2017) 128:1353–1358
DOI 10.1007/s10973-016-6047-9

Thermal properties of europium nitrate hexahydrate $Eu(NO_3)_3{\cdot}6H_2O$

P. Melnikov[1] · I. V. Arkhangelsky[1] · V. A. Nascimento[1] · L. C. S. de Oliveira[1] · A. F. Silva[1] · L. Z. Zanoni[1]

Received: 29 April 2016 / Accepted: 9 December 2016 / Published online: 28 December 2016

Abstract The hexahydrate of europium nitrate hexahydrate $Eu(NO_3)_3{\cdot}6H_2O$ shows no phase transitions in the range of −40 to 76 °C when it melts in its own water of crystallization. It was shown that the thermal decomposition is a complex step-wise process, which starts with the simultaneous condensation of 6 mol of the initial monomer $Eu(NO_3)_3{\cdot}6H_2O$ into a cyclic cluster $6[Eu(NO_3)_3{\cdot}6H_2O]$. This hexamer gradually loses water and nitric acid, and a series of intermediate amorphous oxynitrates is formed. The removal of HNO_3 azeotrope is essentially a continuous process occurring in the liquid phase. At higher temperatures, oxynitrates undergo further degradation, lose water, nitrogen dioxide, and oxygen, and finally, after having lost lattice water, are transformed into europium oxide. All mass losses are satisfactorily accounted for under the proposed scheme of thermal decomposition.

Keywords Rare earth · Europium nitrate hexahydrate · Thermal decomposition · Oxynitrates

Introduction

The development of new optoelectronic devices depends not only on materials engineering at a practical level, but also on a clear understanding of the precursor's properties and fundamental science behind these properties. This stimulates the research dedicated to terbium and europium as luminescent probes. Moreover, europium is a unique activator that gives both the broad-band and narrow-band emissions depending on its valences (+2, +3, and +4) [1]. It may seem paradoxical, but the data referring to a relatively common compound $Eu(NO_3)_3{\cdot}6H_2O$, frequently used as a starting material for numerous syntheses of luminescent materials, are limited. Europium nitrate hexahydrate [tetraaquatrinitratoeuropium(III) dihydrate] belongs the triclinic space group *P1* with $Z = 2$. The inner coordination shell (Fig. 1) contains central europium atom and four water molecules at the distances from central atom in the range 2.379–2.933 Å. The second coordination shell consists of two lattice water molecules at the distances 4.527 and 4.545 Å [2]. Such geometry suggests a complex, multi-step character of thermal decomposition.

Broadly speaking, the decomposition of rare earth nitrates is not a simple process of water removal. The stability of rare earth octahedral complex cations is so high that part of NO_3 groups present in these structures are eliminated before a complete dehydration is achieved or at least simultaneously with this process. In this context, the conclusions drawn from the thermal decomposition kinetics of the alleged "dehydrated" nitrates [3] are questionable when the compounds are obtained using a technique that, in principle, would not have allowed preparing anhydrous salts. More recent investigations have been extended to thermal decomposition of lanthanide nitrates $Ln^{III}(NO_3)_3{\cdot}xH_2O$, where Ln^{III} = Pr, Y, Cr, Al, Fe, Sm, Gd, Dy [4–12], as well as nitrates of Ga^{III} [13] and Sc^{III} [14], establishing that all attempts to prepare the anhydrous compounds under hydrothermal conditions were unsuccessful. As in the case of organic lanthanide derivatives [15], the final products are sesquioxides Ln_2O_3.

✉ P. Melnikov
petrmelnikov@yahoo.com

[1] Federal University of Mato Grosso do Sul, Campo Grande, Mato Grosso do Sul, Brazil

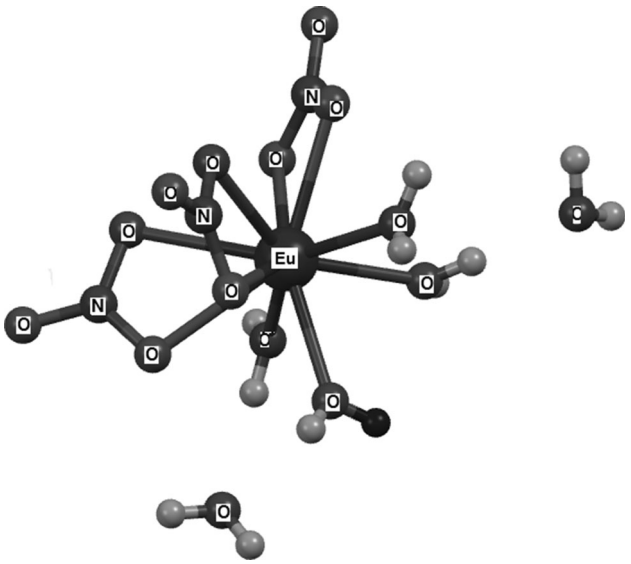

Fig. 1 Coordination scheme of $Eu(NO_3)_3{\cdot}6H_2O$

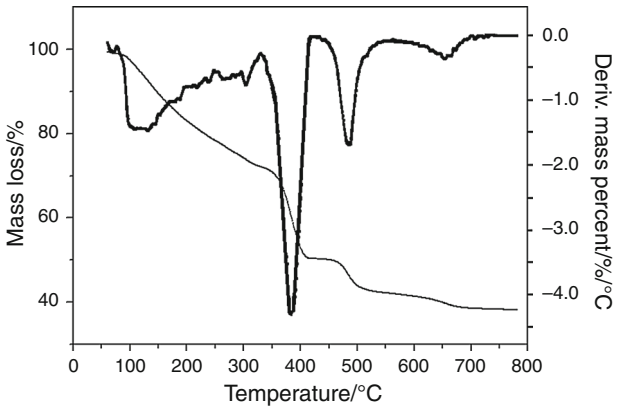

Fig. 3 TG curve of $Eu(NO_3)_3{\cdot}6H_2O$

Materials and methods

The starting reagent used was europium nitrate hexahydrate $Eu(NO_3)_3{\cdot}6H_2O$, of analytical grade purity (99.9%), purchased from Sigma-Aldrich. Direct heating of the commercial reagent resulted in mass loss of 61.5% confirming the water number six (calc. 61.4%). Thermal gravimetric analysis (TG, temperature range 25–800 °C) and differential scanning calorimetry (DSC, temperature range −40 to 600) were used to study thermal behavior, employing a Netsch STA Jupiter 449C Instrumentation. Test specimens were heated in a flux of argon, always at a heating rate 5 °C min^{-1}. Mass losses during heating were analyzed and compared to previously calculated values. Melting point, gas liberation, and crystallization processes were additionally monitored by visual observation, allowing the visualization of NO_2 vapors, and other peculiarities. The evolution of volatiles was measured using a Netsch STA Jupiter 449C apparatus coupled with a FTIR Tensor 27 Bruker spectrometer. The spectra were detected in a range 400–4000 cm^{-1}. Temperature of the transport gas line was 240 °C. The spectra were taken for 12 s at a frequency accuracy of 1 cm^{-1}. The identification of the spectra was done on the basis of NIST Chemistry WebBook [16]. The samples were sealed in glass ampoules in a hot condition in order to avoid the impact of water vapors from the air. X-ray powder patterns of solid samples (CuKα radiation) were registered with a Siemens Kristalloflex diffractometer with a graphite diffracted beam monochromator and Ni filter. Data were collected in the range of $2\theta = 10°$–$70°$ with a scan step $2\theta = 0.02°$ and scan rate of 18 min^{-1}. Phase identification was performed using ICDD PDF-2 database.

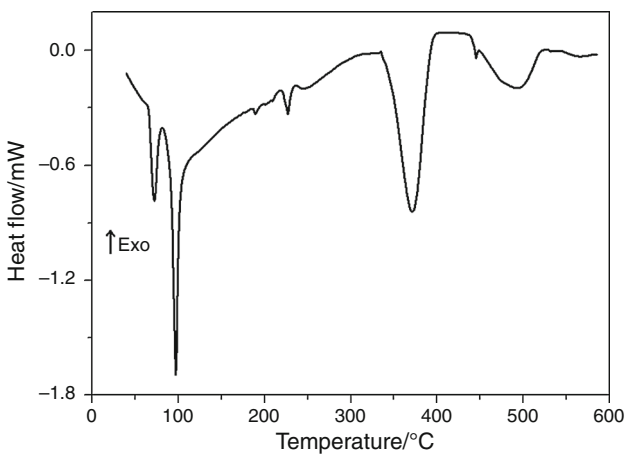

Fig. 2 DSC curve of $Eu(NO_3)_3{\cdot}6H_2O$

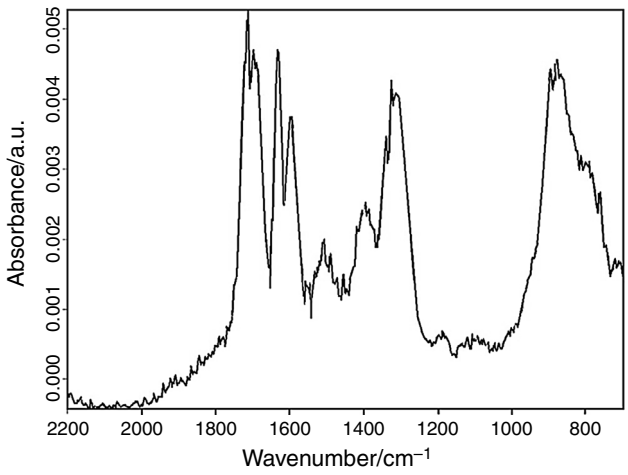

Fig. 4 IR spectrum of the volatile products corresponding to 280 °C

Results and discussion

As established by visual observations, the compound turns into a clear liquid at around 65 °C similar to other nitrate hexahydrates. This liquid begins to boil at ~112 °C, and immediately, the smell of gaseous HNO_3 starts to feel. The solidification/crystallization process becomes noticeable at ~215 °C, and then from ~328 °C on nitrogen dioxide fumes are released.

The DSC analysis of $Eu(NO_3)_3{\cdot}6H_2O$ is presented in Fig. 2. No solid–solid phase transition was found, at least over −40 °C. From approximately 50 °C on, sharp endothermic effects become evident, neatly reflecting the onset of decomposition processes. Along with TG pattern, their analysis can be used for a rigorous interpretation of results.

The representative TG curve of $Eu(NO_3)_3{\cdot}6H_2O$ is shown in Fig. 3. It can be seen that despite the obvious similarities with $Dy(NO_3)_3{\cdot}6H_2O$ from our recent publication [11], they differ markedly, since at the early stages of thermal decomposition mass losses of $Eu(NO_3)_3{\cdot}6H_2O$ are not adequately resolved. That is why the interpretation of dysprosium effects could not be transferred straightforwardly to europium compound. In this case, we had to be guided exclusively by the endothermic peaks of the aforementioned DSC curve. So, the two initial mass losses (1.4 and 2.9%) are due to water evaporation after fusion of the original hexahydrate at 76–78 °C (total 7 mol). This temperature is also confirmed by direct visual observation, when the melt loses gas bubbles and turns into a clear yellow liquid. Our working hypothesis was that europium nitrate is hydrolyzed by the hot crystallization water, and as a result nitric acid should have been produced. Indeed, this acid, or rather the azeotrope 68% HNO_3–32% H_2O (boiling point 120.5 °C), is detected by the IR sensor of the volatile products from the very beginning of the thermal treatment. Nitric acid is identified by its characteristic absorption bands at 892, 1319, 1508, 1596, 1631, and 1716 cm^{-1} (Fig. 4). It is clearly seen that the two releases of nitric acid are accompanied by net endothermic effects on DSC curve, with onsets at 242 and 316 °C, respectively. The 3D diagram of IR spectrum shown in Fig. 6 gives a general view of absorption at sequential temperatures (Fig. 5).

At this step, we do not have the ability to judge about precise compositions, since the mixture is in the liquid state, and the removal of HNO_3 is essentially a continuous process. This is confirmed by dynamics of nitric acid removal in relation to TG curve (Fig. 6). It would be reasonable to assume that the pyrolysis curve shows the presence of various chemical products, not a single stoichiometric compound of definite composition. At temperatures above 200 °C, melt becomes viscous and then solidifies at ~250 °C. The X-ray powder diagram does not show the presence of crystalline products. Unfortunately, amorphous oxynitrate(s) cannot be unambiguously identified by means of IR spectra due to the overlapping bands of nitrate ion and water.

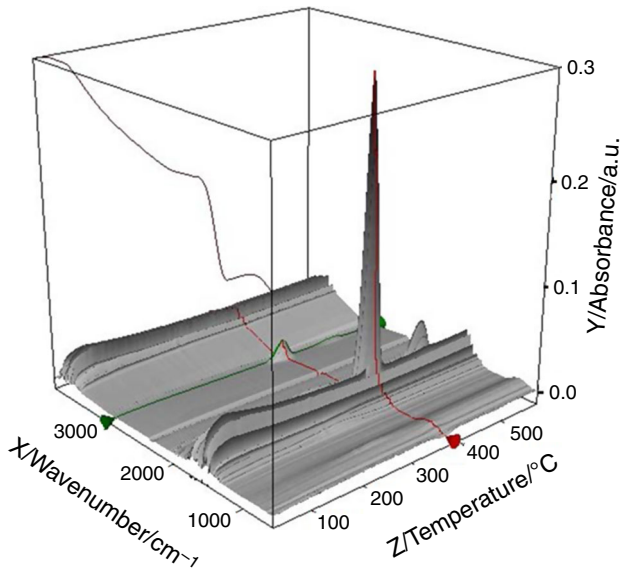

Fig. 5 Temperature-dependent 3D diagram of IR spectra of the $Eu(NO_3)_3{\cdot}6H_2O$ thermal decomposition

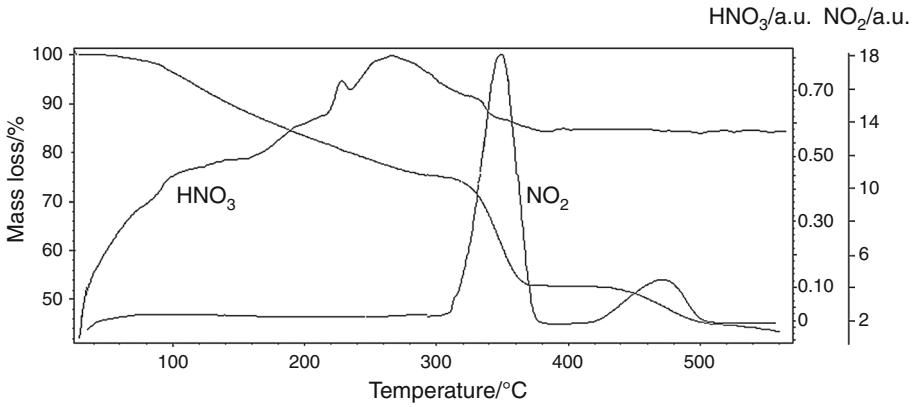

Fig. 6 Dynamics of HNO_3 (**a**) and NO_2 (**b**) removal in relation to TG curve

However, we must bear in mind that the early stages of thermal decomposition comprise at least two processes that occur simultaneously: dehydration and hydrolysis of europium nitrate hexahydrate by the water from the distant coordination shell that is the water of crystallization. It is important that the former process is substantially independent on temperature, while the latter is characterized by fast kinetics, leading to recombination of ligands in closer coordination shell. That is why a number of rare earth lower hydrates could have been isolated at room temperature after prolonged desiccation over concentrated H_2SO_4. At the next step, between 78 and 229 °C the compound loses 19.4% of mass which corresponds to the evaporation of $14H_2O$ and $4HNO_3$.

Upon further heating, only two mol of HNO_3 are removed and then the composition of the gaseous phase changes. The observation of the characteristic brown color of nitrogen dioxide at 328 °C and the known instability of HNO_3 at high temperatures suggests that the acid in its molecular form is not actually present. This is confirmed by dynamics of nitric acid release in relation to TG curve given in Fig. 6. The thermal decomposition of nitric acid represents a reversible endothermic reaction and almost quantitatively produces H_2O, NO_2, and oxygen [17]. At this step, the mass loss is 20.9% corresponding to $10NO_2$ and 5O. The presence of nitrogen dioxide at this temperature was further confirmed by the IR spectrum of volatile products showing the characteristic bands at 1,314, 1,595, and 1629 cm^{-1} (Fig. 7). Oxygen in principle cannot be registered by this technique due to the lack of changing dipole moment.

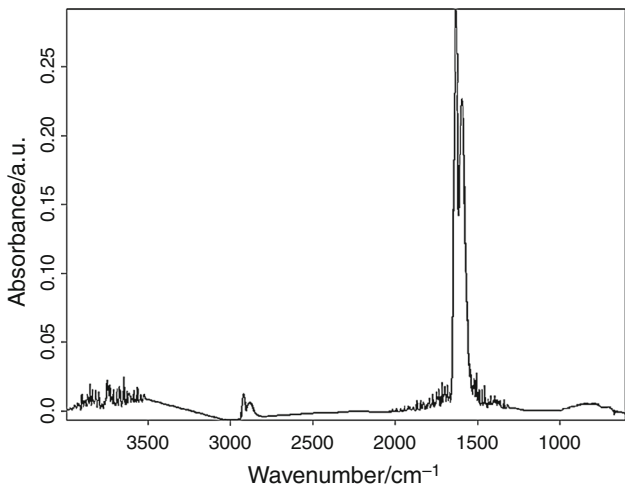

Fig. 7 IR spectrum of the volatile products corresponding to 380 °C

At the next step, $2NO_2$ and 1O (mass loss 8.6%) are lost. This suggests a mechanism involving N_2O_5 formation with immediate disproportionation into nitrogen dioxide and oxygen. The curves of simultaneous equilibrium of NO, NO_2, N_2O_3, and N_2O_4 [18] show that above 300 °C nitrogen dioxide is the only existing phase. Then denitrification is complete, and only a hydrated europium oxide remains. Finally, the latter will lose 6 mol of water and be transformed into $3Eu_2O_3$ with total mass loss 61.5%. It can be seen (Table 1) that the experimental mass losses actually correspond to the values calculated for each stage.

It is obvious that the loss of mass which takes place during the first stages cannot possibly result from the disintegration of the single mol of $Eu(NO_3)_3{\cdot}6H_2O$, if only because it contains no more than one atom of metal, whereas at least two are required for the formation of Eu_2O_3. Consequently, we must take into consideration the process of condensation, characteristic of the chemistry of cations with the charge +3. Here, it is worth referring to the existing published data on the elements whose properties are close to europium. For dysprosium and

Table 1 Mass losses at different stages of $Eu(NO_3)_3{\cdot}6H_2O$ pyrolysis and composition of the volatile products in relation to the initial six monomers

Compositions	Loss of volatile products/mol				Mass loss/%	
	Water	Nitric acid	Nitrogen dioxide	Oxygen	Exp.	Calc.
[6 $Eu(NO_3)_3$]·$36H_2O$	2	–	–	–	1.4	1.34
[6 $Eu(NO_3)_3$]·$34H_2O$	5	–	–	–	4.3	4.70
[6 $Eu(NO_3)_3$]·$29H_2O$	14	4	–	–	23.7	23.53
$Eu_6(NO_3)_{14}O_2{\cdot}13H_2O$	–	2	–	–	27.8	27.57
$Eu_6(NO_3)_{12}O_3{\cdot}12H_2O$	–	–	10	5	48.7	48.86
$Eu_6(NO_3)_2O_8{\cdot}12H_2O$	6	–	2	1	57.3	56.43
$Eu_6O_{18}{\cdot}6H_2O$	6	–	–	–	61.5	61.43
3 Eu_2O_6						

Total: $33H_2O$, $6HNO_3$, $12NO_2$, 6O

Final product: $3Eu_2O_6$

samarium, for example, it has been shown that such condensation leads to the formation of stable groups containing six metal atoms [11, 12]. This can be also true for gadolinium nitrate [6] as the data allow a double interpretation. As to europium itself "polymeric cluster" containing six metal atoms, of the composition $[Eu_6O(OH)_8(H_2O)_{12}(NO_3)_6](NO_3)_2{\cdot}6H_2O$ has been isolated in solid form and its structure studied [19]. It was early obtained in the form of single crystals by heating of a clear solution of europium oxide in an excess of concentrated nitric acid, until decomposition started. The melt was treated with ethyl alcohol and water, after which fine precipitate was collected. As practically all of these clusters contain six lanthanide atoms, it was reasonable to consider the condensation of at least six monomer units $Eu(NO_3)_3{\cdot}6H_2O$.

Calculations show that the hypothesis concerning cluster preexistence in the solid nitrate hydrates is quite applicable to the present case of europium nitrate hydrate. Indeed, that suggests that in the condensation process at least 6 mol of $[Eu(NO_3)_3{\cdot}6H_2O]$ are involved, and the overall decomposition can be described as:

$$6\,[Eu(NO_3)_3{\cdot}6H_2O] = 3Eu_2O_3 + 6HNO_3 + 12NO_2 + 3O_2 + 33H_2O \quad (1)$$

Naturally, we might start considering the condensation of two units, as in the case of aluminum nitrate octahydrate [7] or four units like in the case of scandium nitrate but, at the end of the process, one would have to resort to unaccountable fractional values of stoichiometric coefficients.

Conclusions

1. The hexahydrate of europium nitrate hexahydrate $Eu(NO_3)_3{\cdot}6H_2O$ shows no phase transitions in the range of −40 to 76 °C when it melts in its own water of crystallization.
2. It was shown that the thermal decomposition is a complex step-wise process, which starts with the simultaneous condensation of 6 mol of the initial monomer $Eu(NO_3)_3{\cdot}6H_2O$ into a cyclic cluster $6[Eu(NO_3)_3{\cdot}6H_2O]$.
3. This hexamer gradually loses water and nitric acid, and a series of intermediate amorphous oxynitrates is formed.
4. The removal of HNO_3 azeotrope is essentially a continuous process occurring in the liquid phase.
5. At higher temperatures, oxynitrates undergo further degradation, lose water, nitrogen dioxide, and oxygen, and finally, after having lost lattice water, are transformed into europium oxide. All mass losses are satisfactorily accounted for under the proposed scheme of thermal decomposition.

Acknowledgements The authors are indebted to CNPq and FUNDECT (Brazilian agencies) for financial support.

References

1. Nazarov M, Young ND. New generation of terbium and europium activated phosphors. Boca Raton: Pan Stanford Publishing; 2011.
2. Stumpf T, Bolte M. Tetraaquatrinitratoeuropium(III) dihydrate. Acta Cryst E Struct Rep Online. 2001;57:10–1.
3. Strydom CA, Van Vuuren CPJ. The thermal decomposition of lanthanum(III), praseodymium (III) and europium(III) nitrates. Thermochim Acta. 1988;124:277–83.
4. Hussein GAM, Balboul BAA, A-Warith MA, Othman AGM. Thermal genesis course and characterization of praseodymium oxide from praseodymium nitrate hydtrate. Thermochim Acta. 2001;369:59–66.
5. Melnikov P, Nascimento VA, Consolo LZZ, Silva AF. Mechanism of thermal decomposition of yttrium nitrate hexahydrate $Y(NO_3)_3{\cdot}6H2O$ and modeling of intermediate oxynitrates. J Therm Anal Calorim. 2013;111:115–9.
6. Melnikov P, Nascimento VA, Consolo LZZ. Computerized modeling of intermediate compounds formed during thermal decomposition of gadolinium nitrate hydrate. Russ J Phys Chem. 2012;86:1659–63.
7. Melnikov P, Nascimento VA, Arkhangelsky IV, Consolo LZZ. Thermal decomposition mechanism of aluminum nitrate octahydrate and characterization of intermediate products by the technique of computerized modeling. J Therm Anal Calorim. 2013;111:543–8.
8. Melnikov P, Nascimento VA, Arkhangelsky IV, Zanoni Consolo LZ, de Oliveira LCS. Thermolysis mechanism of chromium nitrate nonahydrate and computerized modeling of intermediate products. J Therm Anal Calorim. 2013;114:1021–7.
9. Wieczorek-Ciurowa K, Kozak AJ. The thermal decomposition of $Fe(NO_3)_3{\cdot}9H_2O$. J Therm Anal Calorim. 1999;58:647–51.
10. Melnikov P, Nascimento VA, Arkhangelsky IV, Zanoni Consolo LZ, de Oliveira LCS. Thermal decomposition mechanism of iron (III) nitrate and characterization of intermediate products by the technique of computerized modeling. J Therm Anal Calorim. 2014;115:145–51.
11. Melnikov P, Arkhangelsky IV, Nascimento VA, Silva AF, Zanoni Consolo LZ, de Oliveira LCS, Herrero AS. Thermolysis mechanism of dysprosium hexahydrate nitrate $Dy(NO_3)_3{\cdot}6H_2O$ and modeling of intermediate decomposition products. J Therm Anal Calorim. 2015;122:571–8.
12. Melnikov P, Arkhangelsky IV, Nascimento VA, Silva AF, Zanoni Consolo LZ. Thermolysis mechanism of samarium nitrate hexahydrate. J Therm Anal Calorim. 2014;118:1537–41.
13. Melnikov P, Nascimento VA, Zanoni Consolo LZ. Thermal decomposition of gallium nitrate hydrate and modeling of thermolysis products. J Therm Anal Calorim. 2012;107:1117–21.
14. Melnikov P, Nascimento VA, Arkhangelsky IV, Silva AF, Zanoni Consolo LZ. Thermogravimetric study of the scandium nitrate hexahydrate thermolysis and computer modeling of intermediate oxynitrates. J Therm Anal Calorim. 2015;119:1073–9.
15. Grivel JC. Thermal decomposition of $Ln(C_2H_5CO_2)_3$ (Ln = Ho, Er, Tm and Yb). J Therm Anal Calorim. 2012;109:81–8.
16. NIST Chemistry WebBook, NIST Standard Reference Database Number 69. www.http//webbook.nist/chemistry. Accessed 21 April 2016.

17. Manelis GB, Nazin GM, Rubtsov YuT, Strunin VA. Thermal decomposition and combustion of explosives and propellants. Boca Raton: CRC Press; 2003.
18. Bibart CH, Ewing GE. Vibrational spectrum of gaseous N_2O_3. J Chem Phys. 1974;61:1293–9.
19. Giester G, Zak Z, Unfried P. Synthesis and crystal structure of rare earth basic nitrates hydrates Part III, $[Ln_6O(OH)_8(H_2O)_{12}(NO_3)_6](NO_3)_2\ xH_2O$, Ln = Y, Sm, Eu, Gd, Tb, Dy, Ho, Er, Tm, Yb, Lu; x = 3, 4, 5, 6. J Alloy Compd. 2009;481:116–28 **(and references therein)**.